Supporting Information For Online Publication

Supplement A: The Narrative Indicators

Capital Requirements

1981/15/12 Tightening

The Federal Reserve Board and the Office of the Comptroller of the Currency introduce capital standards common to all banks. The standards employ a leverage ratio of primary capital (which consisted mainly of equity and loan loss reserves) to average total assets. Standards differ slightly by type of institution, with a value of 6 % for community banks and 5 % for large regional institutions. Source: Federal Deposit Insurance Corporation (FDIC).

1983/03/01 Tightening

Congress passes the International Lending Supervision Act (ILSA). This statute directs the banking regulators to "achieve and maintain adequate capital by establishing minimum levels of capital" for banks subject to regulation. The ILSA was enacted in response to the Latin American debt crisis, which revealed a high risk of the foreign sovereign debt exposure of some U.S. banks. The law also put on firmer footing the regulators' authority to issue capital adequacy rules. Source: Federal Register.

1985/15/06 Tightening

Regulators abolish the differences in bank leverage by type of bank as established in the 1981/15/12 Act in favour of a uniform standard of 5.5 %. Banks with less than 3% of primary-capital-to-total assets are declared to be "operating in unsafe condition" and are made subject to enforcement actions. Source: FDIC.

1990/31/12 Tightening

The first stage of the Basel I rules is enacted by U.S. regulators imposing two requirements on capital ratios, related to Tier 1 and Tier 2 capital. First, Basel I calls for a minimum ratio of total (Tier 1 plus Tier2) capital to risk-weighted assets (RWA) of 8 %, and of Tier 1 capital to risk-weighted assets of 4 %. The first stage requires respective ratios of 7.25% and 3%, while the full are phased in until the end of 1992. Source: Posner (2014).[1]

1991/19/12 Tightening

The Federal Deposit Insurance Corporation Improvement Act categorises institutions according to their capital ratios. Other than "well capitalised" banks (at least 10 % total risk-based, 6 % Tier 1 risk-based, and 5% leverage capital ratios) face restrictions on certain activities and are subject to mandatory or discretionary supervisory actions. Source: Government Publishing Office (GPO).

1992/31/12 Tightening

The final implementation stage of the Basel I rules is enacted by U.S. regulators with the own funds ratio set to 8%, and the leverage ratio set to 4%. Source: Posner (2014).

[1]Posner, E. (2014). How do bank regulators determine capital adequacy requirements? Coase-Sandor Institute for Law & Economics Working Paper 698.

2002/01/01 Easing

The Recourse Rule reduces risk weights for AAA- and A.A.- rated "private-label" mortgage-backed securities (MBS) and collateralised debt obligation (CDO) tranches originated by large banks to 0.2 in line with government-sponsored enterprise (GSE)–originated MBS. For A-rated tranches, the risk weights are set to 0.5, while lower-rated tranches are assigned higher risk weights. The rule is designed to encourage securitisation without encouraging risk-taking, while risk weights are kept close to 2004 Basel II risk weights. Source: Posner (2014).

2006/31/12 Tightening

The Tier 1 leverage ratio is increased to 4 %. Source: Posner (2014).

2013/01/01 Tightening

The Federal Reserve Board approves a final rule to implement changes to the market risk capital rule, which requires banking organisations with significant trading activities to adjust their capital requirements to better account for the market risks of those activities (Basel II.5). The adoption of Basel II.5, also known as the market capital risk rule, has been issued by the U.S. federal banking regulators on June 7, 2012. Source: Federal Reserve Board (FRB).

2013/30/07 Tightening

The Federal Reserve Board (FRB) introduces a supplementary leverage ratio requirement of 3% for banks using the advanced approach for RWA calculation. An additional 2% buffer requirement has been proposed for G-SIBs. Further, IRB banks are required to apply the lower of capital ratios calculated under the standardised and IRB approaches. Source: FRB.

Mortgage Underwriting Standards

1958/01/04 Easing

Changes to requirements on loans insured by the Veteran Administration. Removal of 2% down payment requirement on insured loans. Act of Congress changes requirements on loans insured by the Federal Housing Administration. (i) LTV for new construction, 97% of first $ 13,500 of value plus 85% of next USD 2,500 plus 70% of value in excess of $ 16,000 to maximum mortgage of USD 20,000. (ii) LTV for existing construction, 90% of first US$D 13,500 of value plus 85% of next $ 2,500 plus 70% of value in excess of $ 16,000 to maximum mortgage of $ 20,000. Source: Elliot et al. (2013).

1959/23/09 Easing

Act of Congress changes requirements on loans insured by the Federal Housing Administration. (i) LTV for new construction, 97% of first $ 13,500 of value plus 90% of next $4,500 plus 70% of value in excess of $18,000 to maximum mortgage of $ 22,500. (ii) LTV for existing construction, 90% of first $18,000 of value plus 70% of value in excess of $18,000 to maximum mortgage of $ 22,500. Source: Elliot et al. (2013).

1961/30/06 Easing

Act of Congress changes requirements on loans insured by the Federal Housing Administration. (i) LTV for new construction set to 97% of first $15,000 of value plus 90% of next $5,000 plus 75% of value in excess of $20,000 to maximum mortgage of $25,000. (ii) LTV for existing construction, 90% of first $20,000 of value plus 75% of value in excess of $20,000 to maximum mortgage of $25,000. (iii) Easing of maturity standards for new construction, maximum mortgage term raised from 30 to 35 years or 3/4 of the remaining life of improvements, whichever is less; existing construction still 30 years. Source: Elliot et al. (2013).

1964/01/01 Easing

National banks are allowed to extend real estate loans with 25-year terms and 80% LTV if fully amortised. Source: Elliot et al. (2013).

1964/02/09 Easing

Act of Congress changes requirements on loans insured by the Federal Housing Administration. (i) LTV for new construction, 97% of first $15,000 of value plus 90% of next $5,000 plus 75% of value in excess of $20,000 to maximum mortgage of $30,000. (ii) LTV for existing construction, 90% of first $20,000 of value plus 75% of value in excess of $20,000 to maximum mortgage of $30,000. Source: Elliot et al. (2014).

1965/10/08 Easing

Act of Congress changes requirements on loans insured by the Federal Housing Administration. (i) LTV for new construction, 97% of first $15,000 of value plus 90% of next $5,000 plus 80% of value in excess of $20,000 to maximum mortgage of $30,000. (ii) LTV for existing construction, 90% of first $20,000 of value plus 80% of value in excess of $20,000 to maximum mortgage of $30,000. Source: Elliot et al. (2013).

1970/01/01 Easing

National banks are allowed to extend real estate loans with 30-year terms and 90% LTV if fully amortised. Source: Elliot et al. (2013).

1974/01/01 Easing

National banks are allowed to extend real estate loans with 30-year terms and 90% LTV if 75% amortised. Source: Elliot et al. (2013).

1983/01/09 Easing

LTV limits are removed for all bank mortgage loans (Garn-St Germain). Source: Elliot et al. (2013).

2014/30/01 Tightening

A New Ability to Repay (ATR) and Qualified Mortgage (Q.M.) Rule by Consumer Financial Protection Bureau (CFPB) establishes a minimum set of underwriting standards in the mortgage market. For qualified mortgages, the borrower must prove a debt service-to- income ratio no greater than 43%. Source: CFPB.

Supplement B.1: Linear Discriminant Analysis

This Supplement outlines the relation of the *DC* regression to discriminant analysis, following Maddala (2013).

Consider a dichotomous variable z_t that takes the value $z_t^* = 1$ for m observations and $z_t^* = 0$ for the remaining $T - m$ observations. The objective of discriminant analysis is to estimate function $\psi(x_t)$ to predict z_t^* from a set of random variables $x_t = (x_{1,t}, \ldots, x_{n,t})$ based on the rule $\hat{z_t^*} = 1$ if $\psi(x_t) > 0$ and $\hat{z_t^*} = 0$ otherwise (e.g. Maddala, 2013: 79ff). $\psi(x_t)$ is chosen to minimise the objective function

$$C = C_1 \int_{R_1} f_1(x_t)dx + C_0 \int_{R_0} f_0(x_t)dx,$$

where $f_k(x_t)$ denote the conditional distributions of $x_t|z_t^* = k$. R_1 defines the region such that $\psi(x_t) > 0$ if $x_t \in R_1$ and R_0 is the complement of R_1. C_k is the cost of misclassifying a member of group G_k.

Under the assumption that $x_t|z_t^* = 1 \sim N(\mu_1, \Sigma)$ and $x_t|z_t^* = 0 \sim N(\mu_0, \Sigma)$, the optimal discriminant function is linear, $\psi(x_t) = \psi_1^T x_t$. Under the specific loss function $mC_1 = (T - m)C_0$, the maximum likelihood estimate of parameter vector ψ_1 maximizes the ratio of the squared difference in means between groups and the variance within groups, $(\psi_1^T \Sigma \psi_1)^{-1} \left[\psi_1^T(\mu_1 - \mu_0)\right]^2$. This is equivalent up to scale to estimating a via OLS from the regression $z_t^* = a_0 + a^T x_t + \xi_t$, where $z_t^* = z_t - m/T$ (Maddala, 2013:18ff).

Supplement B.2: Further Details on the Structural VAR

Identifying Restrictions

Section 2 specifies the identifying conditions (3) in terms of conditional expectations, whereas the literature typically defines them in terms of covariances (e.g. Stock and Watson, 2018) as

$$\begin{aligned} \mathrm{cov}(\theta_t, z_t) &> 0 \\ \mathrm{cov}(\epsilon_t, z_t) &= 0. \end{aligned} \tag{10}$$

This section shows that the two specifications are equivalent in the case of a binary instrument. To see this, note that the covariance between a continuous random variable η_t and a binary random variable z_t can be expressed in terms of conditional expectations. For symmetry reasons, it again suffices to show this for a purely binary instrument. Assume, therefore, that z_t is a random variable that takes a value of one with probability $0 < \lambda < 1$ and is zero otherwise. The covariance $\mathrm{cov}(\eta_t, z_t)$ then can be expressed as

$$
\begin{aligned}
\text{cov}(\eta_t, z_t) &= \mathbb{E}(\eta_t z_t) - \mathbb{E}\eta_t \mathbb{E} z_t \\
&= \lambda \mathbb{E}(1\eta_t | z_t = 1) + (1-\lambda)\mathbb{E}(0\eta_t | z_t = 0) - \lambda \mathbb{E}\eta_t \\
&= \lambda \mathbb{E}(\eta_t | z_t = 1) - \lambda \left(\lambda \mathbb{E}(\eta_t | z_t = 1) + (1-\lambda)\mathbb{E}(\eta_t | z_t = 0)\right) \\
&= \lambda(1-\lambda)\left[\mathbb{E}(\eta_t | z_t = 1) - \mathbb{E}(\eta_t | z_t = 0)\right]
\end{aligned}
$$

It follows immediately that conditions (3) imply conditions (10), as $\text{cov}(\theta_t, z_t) = \lambda(1-\lambda)\gamma$ and $\text{cov}(\epsilon_t, z_t) = 0$.

Vice versa, we combine conditions (10) with the assumption that $z_t = 0$ does not convey information about the VAR residuals, $\mathbb{E}(\theta_t|z_t = 0) = \mathbb{E}(\epsilon_t|z_t = 0) = 0$. Hence, $\mathbb{E}(\theta_t|z_t = 1) = [\lambda(1-\lambda)]^{-1}\,\text{cov}(\theta_t, z_t) > 0$ and $\mathbb{E}(\epsilon_t|z_t = 1) = 0$. Conditions (10) therefore imply conditions (3) under the additional assumption. From equation (2)), the assumption $\mathbb{E}(\theta_t|z_t = 0) = \mathbb{E}(\epsilon_t|z_t = 0) = 0$ is equivalent to $\mathbb{E}(u_t|z_t = 0) = 0$, which replaces the standard condition $\mathbb{E}u_t = 0$ in our model. It is, therefore, required as a normalisation condition for identifying the constant term c of the VAR (1), as is obvious from section 2.3 on estimation. Hence, the two specifications are equivalent. Note that conditions (3) do actually not require z_t to be a random variable.

Constructing matrix A_0

Consider the moving average representation of equation (1)

$$
x_t = \left(\sum_{s=0}^{\infty} \Psi_s\right) A_0^{-1} c + \sum_{s=0}^{\infty} \Psi_s A_0^{-1} \varepsilon_{t-s}^{+}
$$

where $(\varepsilon_{t-s}^{+})^T = (\theta_t, \varepsilon_t^T)^T$ and) matrices Ψ_s are the elements of lag polynomial $\Psi(L) = B^{-1}(L)$ with $B(L) = I_n - \sum_{s=1}^{p} B_s L^s$. $\Psi(L)$ defines the IRF of SVAR given by equations (1) and (2). Since $\Psi_0 = I_n$, matrix A_0^{-1} gives the contemporaneous impact of the structural innovations on the VAR series.

We first review the construction of matrix A_0 as, e.g. set out in Arias et al. (2018). The condition $u_t = A_0^{-1}\epsilon_t^{+}$, together with $\mathbb{E}u_t u_t^T = \Sigma$ and $\mathbb{E}\epsilon_t^{+}(\epsilon_t^{+})^T = I_n$, implies $\Sigma^{-1} = A_0^T A_0$. Further, matrix A_0 can be expressed as $A_0^T = A_* Q$, where A_* is a unique lower triangular matrix derived from the Choleski decomposition $\Sigma^{-1} = A_* A_*^T$ and $Q = (q_1, \ldots, q_n)$ is an arbitrary orthogonal matrix, $Q^T = Q^{-1}$, that is constructed such that A_0 satisfies certain restrictions. Arias et al. (2018) show how random draws of Q that satisfy deterministic restrictions may be constructed in a recursive way from a Gram-Schmidt orthogonalisation: column q_j is obtained by drawing an $n \times 1$ vector $x_j \sim N(0, I_n)$ and deriving q_j such that q_j is orthogonal to $(q_1, \ldots, q_{j-1})$ and satisfies further deterministic restrictions specific to innovations $\epsilon_{t,j}^{+}$.

In case of the *DC* restriction, vector α defines the first column of A_0, which implies $q_1 = A_*^{-1}\alpha$. The reverse expression $\alpha = A_* q_1$ is used in case of the SC restriction. An uninformative random draw of α is obtained by drawing q_1 from the Haar measure of orthogonal matrices as $q_1 = v/||v||$, with random draw $v \sim N(0, I_n)$. In both cases, the remaining columns of matrix Q are irrelevant and are constructed without further restrictions, as explained in Arias et al. (2018). Note that q_1 suffices for defining the contemporaneous impact of θ_t, as $A_0^{-1} = (A_*^T)^{-1}Q$ and the first column of A_0^{-1} is therefore well-defined and independent of all q_j with $j > 1$.

Combination with Sign and Zero Restrictions

DC and SC restrictions may also be embedded in the approach of Arias et al. (2018) and thereby be combined with zero and sign restrictions on IRFs. Define $g(A_0, \Psi(L)) = \left[\Psi_0^T, \Psi_1^T, \ldots, \Psi_s^T\right]^T A_0^{-1}$. Express zero and sign restrictions on column j of $\Psi(L)$, i.e. the IRFs to shock $\varepsilon_{j,t}$ as

$$Z_j g(A_0, \Psi(L)) e_j = 0$$
$$S_j g(A_0, \Psi(L)) e_j > 0$$

with appropriate selection matrices Z_j and S_j. Vector e_j denotes column j of identity matrix I_n.

The algorithm of Arias et al. (2018) to generate posterior draws of $\Psi(L)A_0^{-1}$ under this type of restrictions proceeds by (i) drawing from the posterior $(B(L), \Sigma)$ to obtain $\Psi(L)$ and A_*; (ii) obtaining uninformative draws of Q that satisfy the zero restrictions $Z_j g(A_* \Psi(L))$; and (iii) applying an importance sampling step to account for volume changes due to zero restrictions; and (iv) inspecting the validity of sign restrictions.

With the DC regression, the draw of α uniquely defines $q_1 = A_*^{-1}\alpha$, while the remaining columns of Q remain unspecified. The DC restriction may therefore be combined with zero and sign restrictions on shocks $\epsilon_{t,j}$ for $j > 1$. Note that we draw α from a non-degenerate distribution. Hence, there is no volume reduction, and the importance sampling step by Arias et al. (2018) is not required. The SC posterior on shock θ_t is implemented from a rejection sampling step. Hence, it may be combined with sign restrictions on shocks $\epsilon_{t,j}$ for all j and zero restrictions for $j > 1$.

Supplement B.3: Monte Carlo Simulations

For the simulations presented in section 3 of the main text, we set

$$B_1 = \rho \begin{bmatrix} \cos(\omega) & \sin(\psi) \\ -\sin(\psi) & \cos(\psi) \end{bmatrix} \qquad A_0^{-1} = \begin{bmatrix} 1.0 & 0.3 \\ 0.3 & 1.0 \end{bmatrix}^{1/2} \begin{bmatrix} \cos(a) & \sin(a) \\ -\sin(a) & \cos(a) \end{bmatrix}$$

with $\rho = 0.9$, $\psi = 0.2$, and $a = \pi/4$. Matrix B_1 is subject to complex conjugate roots and generates cyclical fluctuations of length of $2\pi/\psi = 32$ quarters. Matrix A_0^{-1} is constructed from the Choleski decomposition times a rotation matrix, $A_0^T = A^* Q$, such that residuals $u_t = A_0^{-1}\varepsilon_t^+$, are subject to a correlation of 0.3 for zero ζ_t, while the rotation matrix ensures that the initial response of $x_{t,1}$ to θ_t is sufficiently large.

To calibrate the number of policy shocks m, we let $\sigma_\nu = 0.01$ and calibrate the expected value of the size of the policy innovation, $\bar{\zeta}$, to achieve the desired expected number of policy interventions m. This give values of $\bar{\zeta} = 1.64$ for $m = 10$ and $\bar{\zeta} = 1.28$ for $m = 20$. As regards simulation (4), since $\operatorname{var} x_{t,i}) = (1 - \rho^2)^{-1}\Sigma_\varepsilon$, with $\omega = 0.5$, the lagged term $x_{2,t-1}$ explains about 70% of the total variance of ζ_t^*. The results presented are based on 1000 draws of the DGP (9) and, for each draw of the DGP, 200 draws of the posterior or bootstrap confidence bounds, respectively. The number of observations is set to $T = 200$.

The Bayesian VARs are explained in the main text. In all cases, we employ an uninformative Jeffrey prior for the reduced form VAR and assume 1 lag in estimation, mirroring the data generating process. For models BV_ζ and BV we skip mean adjustment Γz_t and draw from the proxy regression $\zeta_t = a^T u_t + \xi_t$ using an uninformative Normal-Gamma prior and assuming a normal distribution of residual ξ_t. In implementing the frequentist proxy VAR, we rely on the code of Mertens and Montiel Olea (2018), which offers the bootstraps of Jentsch and Lunsford (2016) and Montiel Olea et al. (2021) for proxy VARs with sparse instruments. The two bootstraps give very similar results, and we report only the latter. For local projections we estimate the equation $x_{1,t+h} = a^T x_t + \gamma_h z_t + u_{1,t}$ and obtain the impulse response to the policy innovation at horizon h directly from coefficient γ_h. We obtain uncertainty bands from a standard bootstrap.

Table B.1 shows the results for an alternative data generating process, which assumes unconditional normality of the generated innovations. In terms of equations (9), this is achieved by setting $\zeta_t \equiv 0$. For strong identification we construct instrument z_t by randomly selecting $m = 10$ observations from the largest 40 realisations of innovations η_t out of $T = 200$ observations. For weak identification, we select them from the $m = 100$ largest realisations. This implies that innovations associated with the instrument are, on average smaller in absolute size in the second case. In either case, however, instrument z_t displays perfect sign concordance with the true innovations η_t for the m selected periods.

The results differ in two important ways from those presented in the main text. First, models DSC and SC using the sign concordance prior with $\lambda = 1$ now provide the most efficient estimates. This suggests that the SC prior is highly efficient under perfect sign concordance. However, model SC continues over-estimating the width of uncertainty bands as it is based on set identification only, whereas model DSC maintains a weak tendency of underestimating them. Second, the Montiel Olea et al. (2021) bootstrap for the frequentist proxy VAR now provides accurate confidence bounds.

Table B.1: Monte Carlo Simulations (alternative DGP)

			BV_ζ	BV	DC	DSC	SC	pV	LP
(1)	Weak	RMSE	.12	.13	.13	.10	.09	.15	.21
		Bias	-.04	-.06	-.06	-.01	-.01	-.05	.05
		IQD	.39	.42	.41	.32	.27	.44	.67
		UB	.41	.52	.51	.23	.25	.55	.97
		Coverage	.79	.85	.84	.65	.71	.85	.89
(2)	Strong	RMSE	.09	.09	.09	.09	.07	.09	.12
		Bias	-.02	-.02	-.04	-.04	-.02	-.03	.06
		IQD	.29	.29	.29	.27	.22	.30	.35
		UB	.26	.27	.28	.29	.53	.32	.48
		Coverage	.72	.74	.75	.76	.98	.78	.85

The table shows statistics of standardised IRFs at horizons $h = 0$ for the alternative data generating process assuming unconditional normality of the residuals as described in the current section of the Supplement. The models are as in the main text. $RMSE$ and $Bias$ are the root mean squared error of the estimate and its difference to the true IRF, respectively. IQD is the [0.1, 0.9] interquantile difference of the distribution of the central estimate measuring its true uncertainty, while UB is the corresponding estimated uncertainty bands. $Coverage$ stands for the share of draws where the true IRF lies within the estimated bands with a correct value of .80.

Supplement B.4: Banking Deregulation Index

Our banking deregulation index is an unweighted average of two sub-indices related to inter-state and intra-state deregulation. Each sub-index takes values of zero (full regulation) to one (no regulation) with intermittent values equal to the GDP shares (as of 1980) of states which had introduced respective deregulation. Hence, the index equals zero before 1970, the beginning of deregulation, and one after 1996.

As discussed by Kroszner and Strahan (1999, 2014), deregulation was a gradual process that consolidated the fragmented banking system in multiple ways. States differed in the timing of when they allowed banks from other states to operate in their jurisdiction and in how many other states were given access. Another source of variation was the timing of the removal of intra-state branching restrictions that prohibited banks from expanding their branch network within a state.[2]

Figure B.1: Banking Deregulation Index

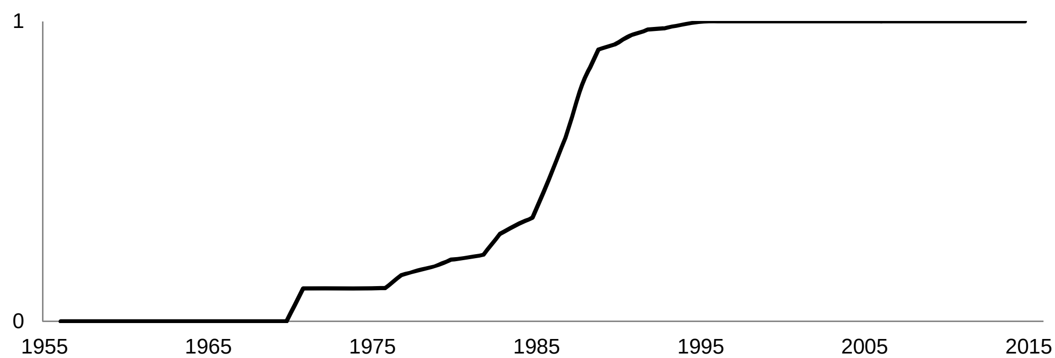

We use the indices provided by Mian et al. (2017), which reflect the start of the deregulation process. For example, the year of inter-state banking deregulation is defined as the first year in which a state allowed out-of-state banks to open a branch. These decisions were based on bilateral arrangements between states until the Riegle-Neal Act of 1994 resulted in the general deregulation of U.S. inter-state banking. Kroszner and Strahan (1999, 2014) conclude that the process of deregulation was largely exogenous to macroeconomic conditions as it was driven by a combination of technological change and shifts in private and public interest. For instance, the speed of deregulation is highly correlated with republican versus democratic state government.

[2]See Kroszner, R.S. and P. E. Strahan. (1999). What Drives Deregulation? Economics and Politics of the Relaxation of Bank Branching Restrictions. The Quarterly Journal of Economics 114(4):1452-1467 and Kroszner, R.S. and P. E. Strahan. (2014). Regulation and Deregulation of the U.S. Banking Industry: Causes, Consequences, and Implications for the Future. In N. L. Rose (ed.). NBER Book Economic Regulation and Its Reform: What Have We Learned?: 485-543. University of Chicago Press.

Figure C.1: Monte Carlo Simulations

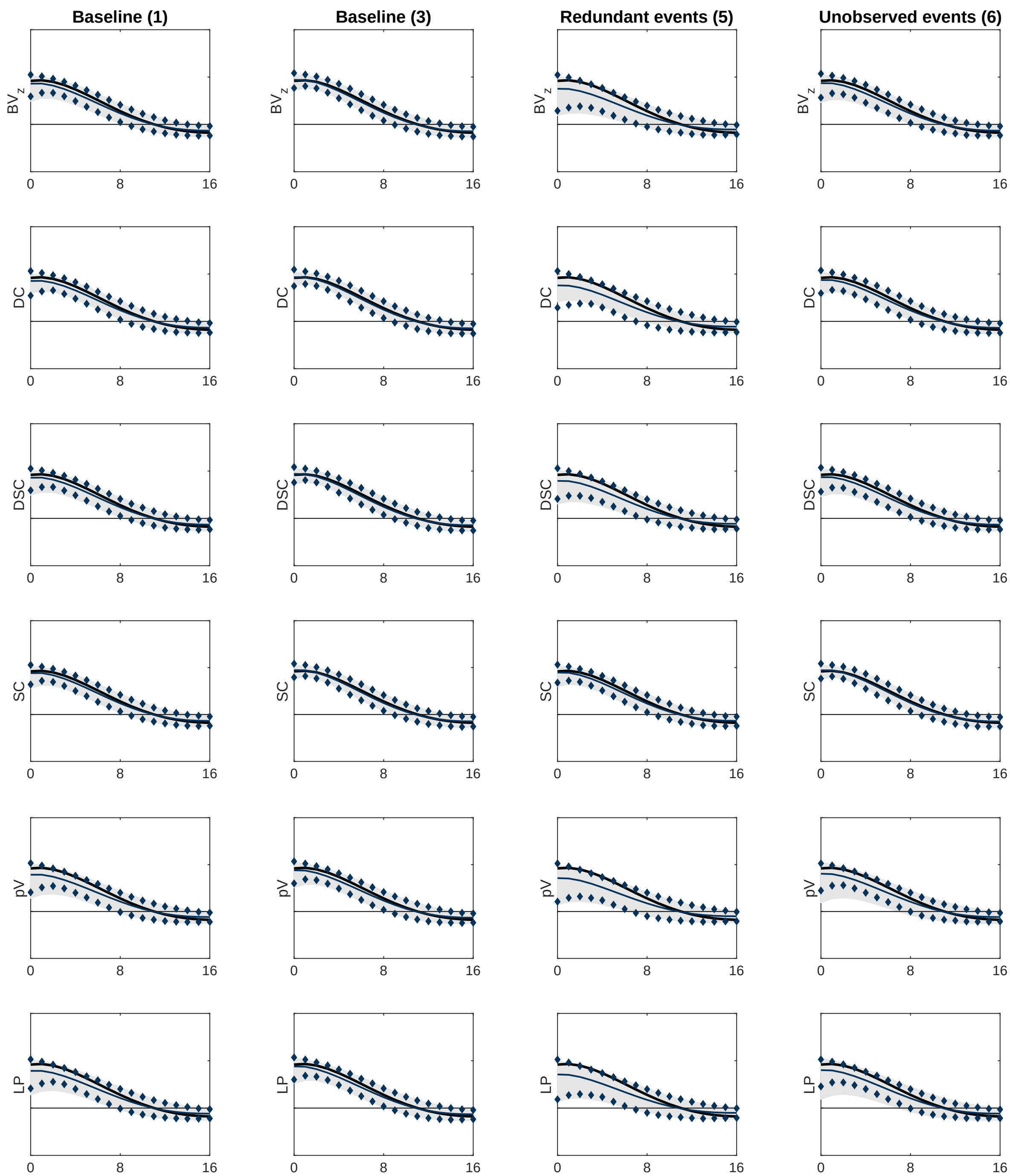

The black solid line shows the true IRF. The blue solid and dotted lines show the central estimate and its [.10, .90] quantiles as provided by the various methods. The shaded area shows the [.10, .90] quantiles of confidence bounds. See Table 1 for the definition of the simulations. The models and the calculation of central estimates and confidence bounds are explained in the main text.

Figure C.2: Standardized IRFs for DC and SC Restrictions

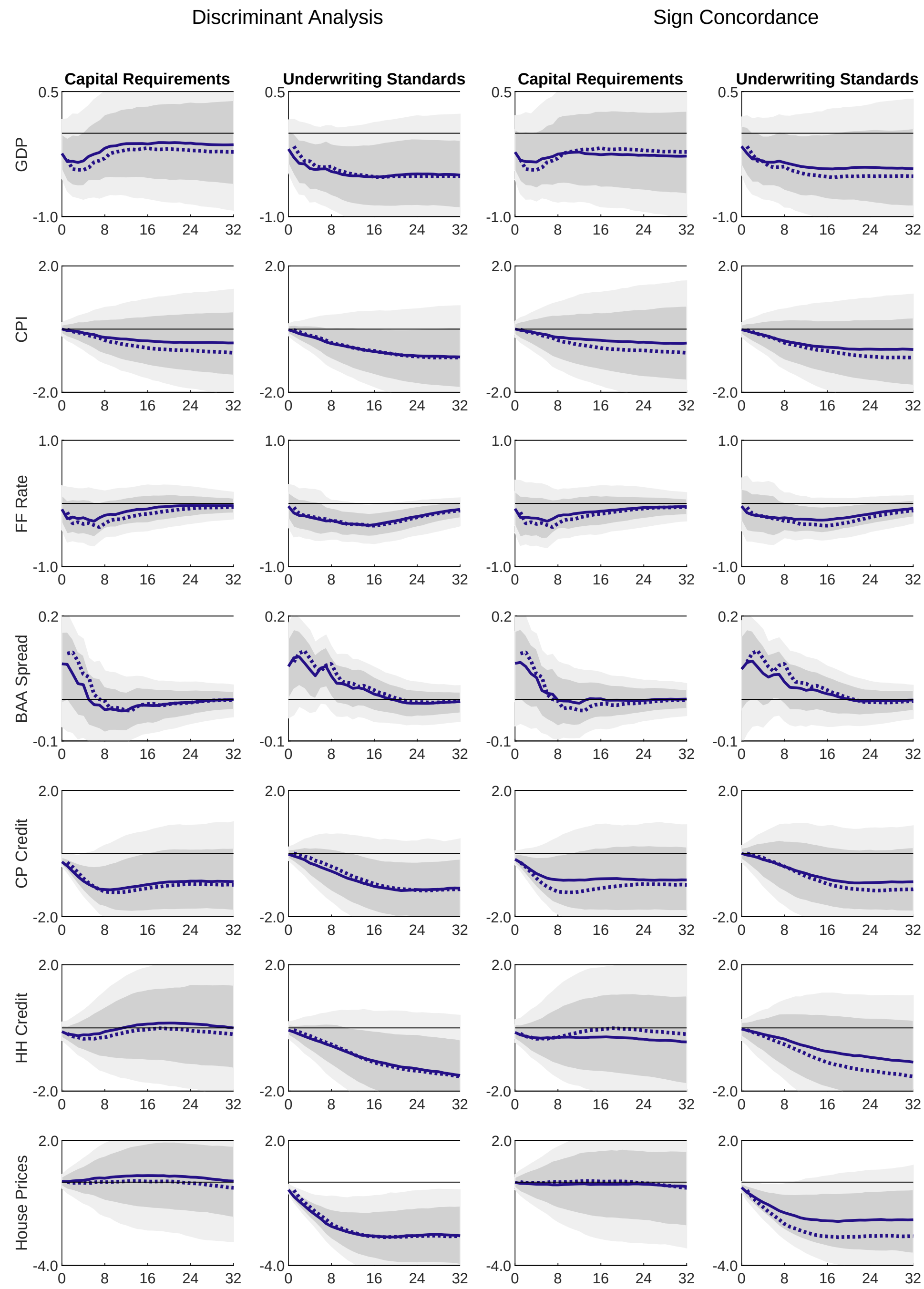

The graphs show the impulse responses to a 1% shock based on either DC or SC restrictions. The solid line shows the median and bounds show [0.05; 0.95] and [0.16; 0.84] quantiles of IRFs. The dotted line shows the main estimate from the DSC restriction.

Figure C.3: IRFs Scaled by the Average Policy Impact

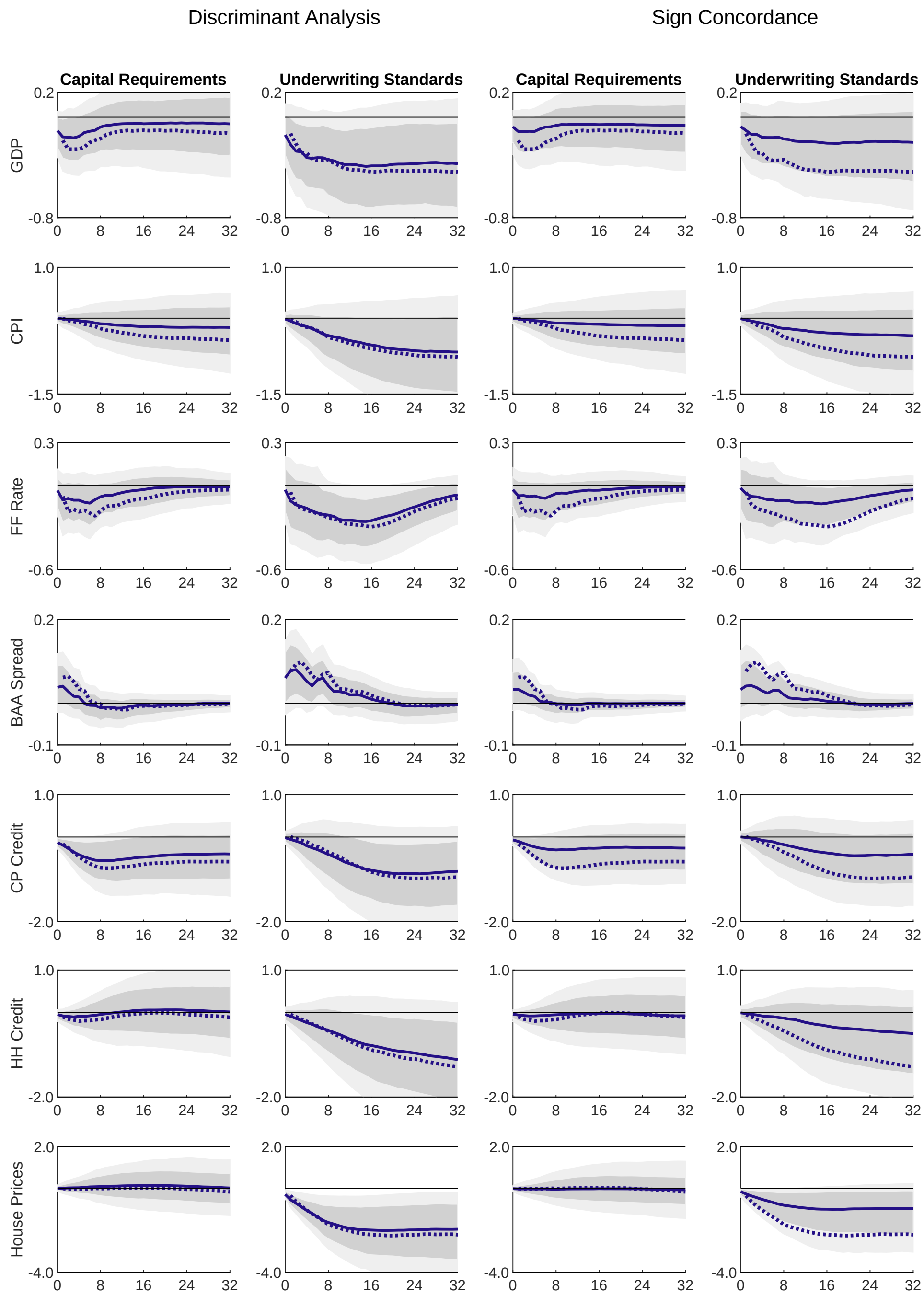

The graphs show the IRFs scaled the impact of average policy shock of size based on either *DC* or *SC* restrictions. See Figure C.3 for further explanations.

Figure C.4: Robustness Check against Lagged Impacts

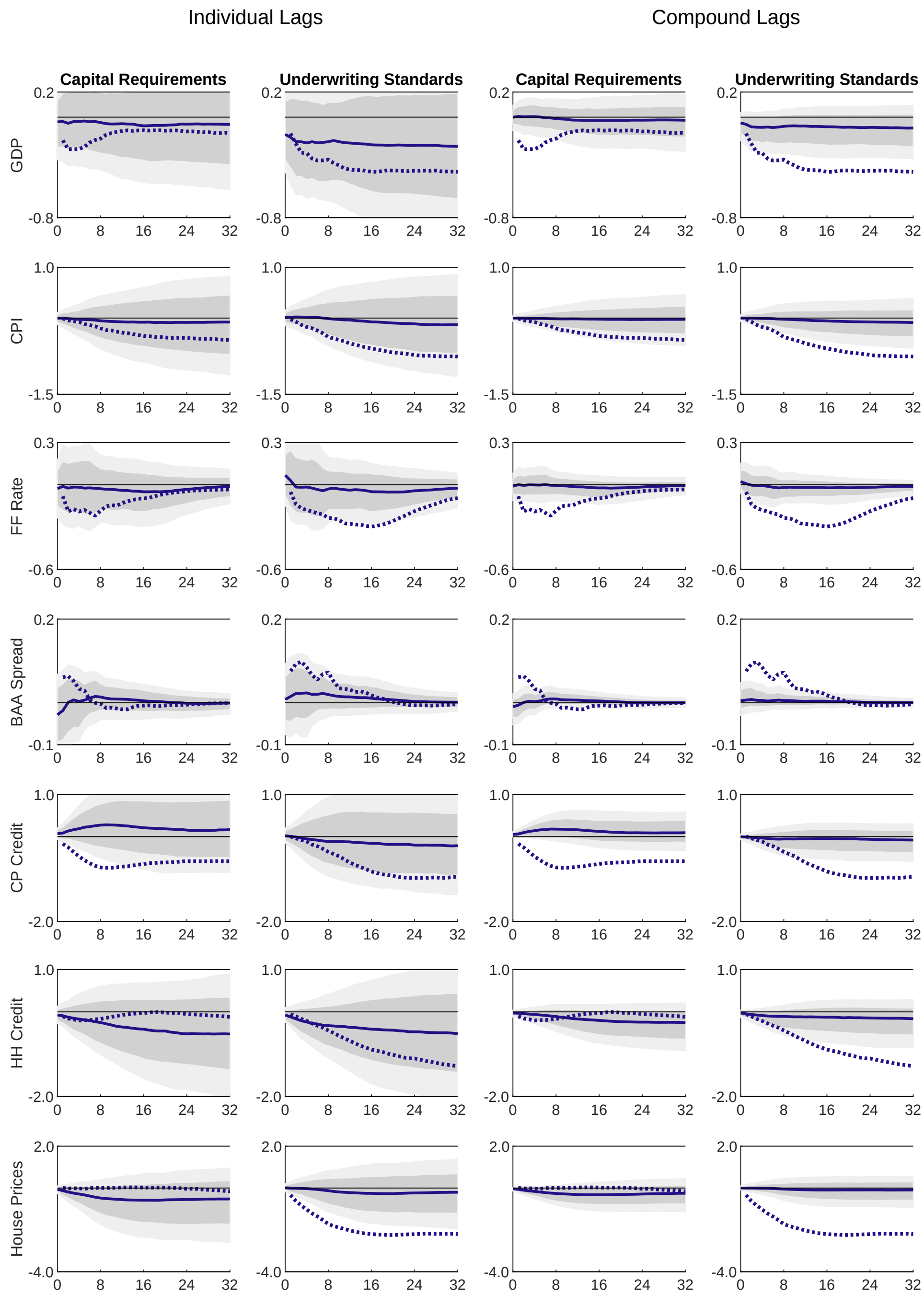

The graphs show standardised IRFs from the robustness checks against lagged innovations discussed in section 4.3. The left-hand graph shows estimates from model *DSC* with lags drawn for individual periods from a uniform distribution; the right-hand one shows estimates from model *DC* for fixed lags from 1 to 4. The latter corresponds to the results shown in Table 4. See Figure C.3 for further explanations.

Figure C.5: Standardized IRFs from Alternative Estimates

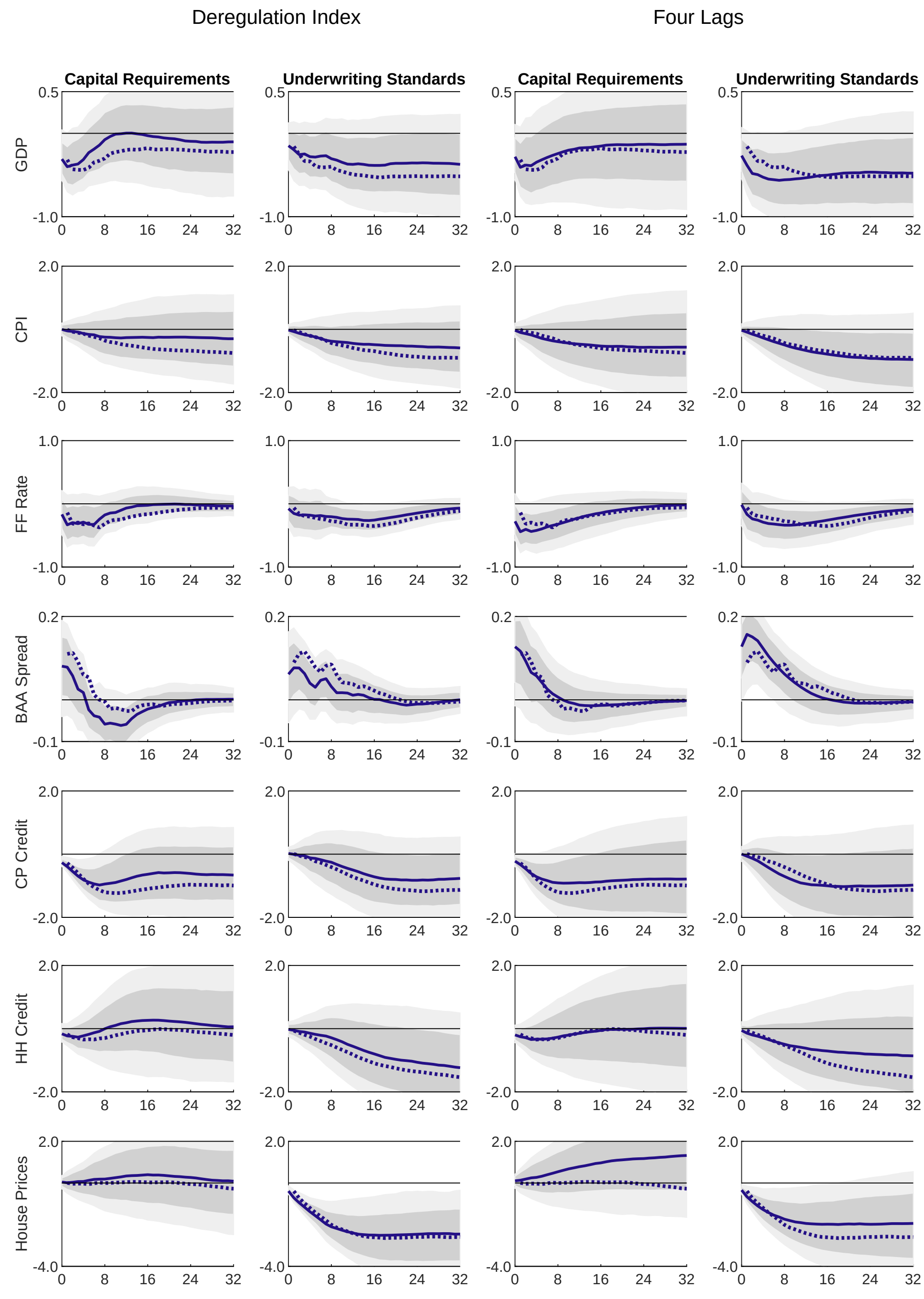

The left-hand graph shows estimates adding the deregulation index. The right-hand graph shows estimates from a VAR with 4 lags. See Figure C.3 for further explanations.

Figure C.6: Standardised IRFs from Standard Proxy VARs

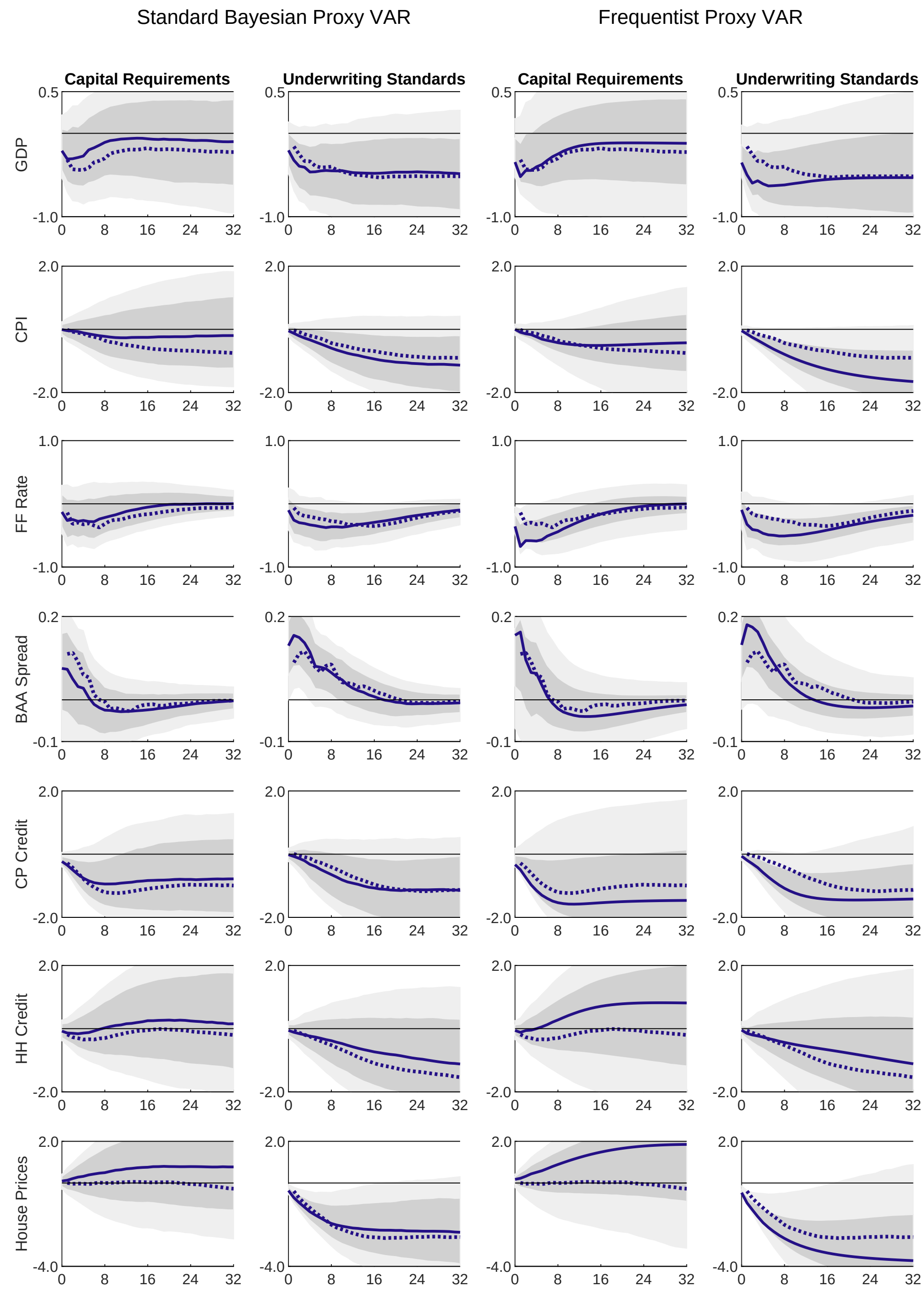

The graphs show IRFs from a standard Bayesian proxy VAR and from a frequentist proxy VAR with confidence bands based on the bootstrap by Montiel Olea et al. (2021). See Figure C.3 for further explanations.